Mechanical Vibrational Relaxation of NO Scattering from Metal and Insulator Surfaces: When and Why They Are Different

Rongrong Yin and Bin Jiang*

Department of Chemical Physics, Hefei National Laboratory for Physical Science at the Microscale, Key Laboratory of Surface and Interface Chemistry and Energy Catalysis of Anhui Higher Education Institutes, University of Science and Technology of China, Hefei, Anhui 230026, China

(Received 12 January 2021; revised 22 February 2021; accepted 16 March 2021; published 14 April 2021)

NO scattering from metallic and insulating surfaces represents contrasting benchmark systems for understanding energy transfer at gas-surface interface. Strikingly different behaviors of highly vibrationally excited NO scattered from Au(111) and LiF(001) were observed and attributed to disparate electronic structures between metals and insulators. Here, we reveal an alternative mechanical origin of this discrepancy by comparative molecular dynamics simulations with globally accurate adiabatic neural network potentials of both systems. We find that highly vibrating NO can reach for the high-dissociation barrier on Au(111), by which vibrational energy can largely transfer to translation or rotation and further dissipate into substrate phonons. This mechanical energy transfer channel is forbidden in the purely repulsive NO/LiF(001) system or for low-vibrating NO on Au(111), where molecular vibration is barely coupled to other degrees of freedom. Our results emphasize that the initial state and potential energy landscape concurrently influence the mechanical energy transfer dynamics of gas-surface scattering.

DOI: 10.1103/PhysRevLett.126.156101

Energy exchange among molecular and surface degrees of freedom (d.o.f.) contributes fundamentally to various physical and chemical phenomena at gas-solid interfaces [1]. Vibrational energy transfer is of particular importance, as vibrational coordinates are intrinsically relevant to forming and breaking of bonds in surface chemical reactions. This has motivated a large body of state-to-state molecular scattering experiments at solid surfaces, demonstrating the most detailed dynamics on how molecular vibration couples with other d.o.f. [2–7]. Such state-resolved data have guided the development of theoretical models toward a predictive understanding of molecule-surface interactions [8–13].

NO scattering from solid surfaces is one of the best studied examples concerning vibrational energy transfer at gas-surface interfaces [14–25], due mainly to the seminal contributions of Wodtke *et al.* [26,27]. One of the most striking observations was the multiquantum vibrational relaxation of highly vibrationally excited NO($\nu_i = 15$) scattered from Au(111) [14], compared to the large vibrational elasticity of NO($\nu_i = 12$) scattered from LiF(001) [23]. This discrepancy was attributed to the contrasting band structures of metals and insulators [14], as the mechanical (electronically adiabatic) gas-surface vibrational relaxation of small molecules was commonly recognized to be inefficient given the mismatch of molecular vibration and surface phonon frequencies [22,28]. That is to say, metals are favorable for electron transfer to NO and efficient vibration-to-electron coupling, while insulators would effectively turn off this electronically nonadiabatic vibrational relaxation channel. This concept was later supported by several different theoretical models [29–33]. In particular, the multistate-based independent electron surface hopping (IESH) model developed by Tully and co-workers [30] qualitatively reproduced the multiquantum vibrational relaxation of NO($v_i = 15$) on Au(111) at a low-incidence energy ($E_i = 0.05$ eV). In comparison, adiabatic dynamics calculations on the same ground state potential energy surface (PES) resulted in large vibrational elasticity [31], as observed in previous experimental [22,23,34] and theoretical [28] findings for NO on LiF(001), implying similarly inefficient mechanical vibrational energy transfer in both systems.

Nevertheless, the IESH model failed to capture some more recently discovered features in the NO/Au(111) system, such as the incidence energy [19,21] and orientation [25] dependence of vibrational relaxation and the final translational energy distributions [21]. These failures were attributed to the inaccuracy of the empirical function parametrized adiabatic PES used in IESH simulations [19], which have been largely remedied by a more accurate machine learned adiabatic NO/Au(111) PES developed by us based on thousands of density-functional theory (DFT) data points [35]. Combining this PES with the orbital-dependent electronic friction tensor accounting for non-adiabatic effects [36], diverse experimental observations have been reasonably reproduced. This new PES predicted a surprisingly large amount of vibrational energy of the highly vibrating NO dissipated mechanically into the gold surface [35], suggesting that the efficiency of mechanical

gas-surface vibrational relaxation is not always low and is very dependent on the adiabatic PES and the underlying electronic structure description. In this Letter, we develop a new high-quality machine learned PES for NO scattering from LiF(001) fit to numerous DFT data. With the state-of-the-art adiabatic PESs for both systems, we are able to elucidate how the observed distinct vibrational inelasticity of NO scattered from metals and insulators is related to their adiabatic PESs and under what conditions the molecular vibrational energy is able to flow into substrate phonons despite the mismatch of their frequencies.

To construct the PES, periodic DFT calculations were performed using the Vienna *ab initio* simulation package vasp [37,38] with the PW91 functional [39]. The LiF(001) surface was modeled with a four-layer slab in a 2×2 supercell, in which the top two layers were movable. The plane wave basis set was truncated at 400 eV and the Brillouin zone was sampled by a $5 \times 5 \times 1$ Monkhorst-Pack k-points mesh. To map out the PES, including both molecular and surface d.o.f., we collected 3608 data points using an adaptive sampling strategy [40] that fully covered the configuration space relevant to highly vibrationally excited NO scattering from LiF(001). Both energies and forces were trained using our recently proposed embedded atom neural network (EANN) approach [41–43]. The NO/Au(111) PES used here was also retrained with EANN using the DFT data in Ref. [35]. To calculate the state-to-state scattering probabilities of NO and account for the large energy exchange between the heavy molecule and the substrate, which is intractable at present by a fully coupled quantum dynamics method, we carried out quasiclassical trajectory (QCT) calculations with the initial and final conditions of NO molecules quantized semiclassically. Such a treatment has shown to be reliable for diatomic scattering from surfaces, e.g., for molecular hydrogen [9], and should work well for a heavier molecule NO with denser vibrational states. More details about the EANN PES and the QCT method (and its validity analysis) are given in the Supplemental Material [44].

Let us first look at the first-principles-determined potential energy landscapes of the NO/Au(111) and NO/LiF(001) systems. As displayed in Fig. 1 and Supplemental Material, Fig. S1 [44], the biggest difference between the two PESs is that NO is dissociative on Au(111) with a high barrier of ~2.86 eV with its bond length elongated to ~1.89 Å, while it is highly repulsive on LiF (001) with its dissociation energy close to that in gas phase (~7.0 eV). Additionally, the NO molecular adsorption energy is higher on Au(111) than on LiF(001) (−0.39 versus −0.06 eV). Accordingly, the NO/Au(111) PES is much more anisotropic and corrugated than the NO/LiF(001) PES, as displayed in Figs. S2–S4 [44]. These differences clearly reflect a stronger interaction of NO with a metal than with an ionic crystal.

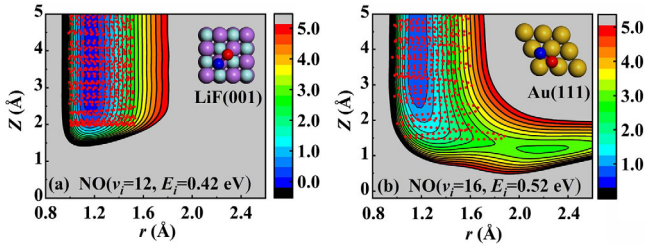

FIG. 1. Two-dimensional cuts of (a) the NO/LiF(001) and (b) the NO/Au(111) PESs as a function of the N-O distance (r) and the molecular height (Z) above the surface, with other coordinates (defined in Fig. S1 [44]) fixed at the adsorption state on LiF(001) and the dissociation transition state on Au(111). A representative trajectory (red dots) of each system is projected on top of the corresponding PES.

Keeping this in mind, we discuss the adiabatic energy transfer dynamics in these two systems in similar conditions. Figure 2 compares the calculated final vibrational state (v_f) distributions of highly vibrationally excited NO molecules scattered from both surfaces, with available experimental data [14,23] at surface temperature (T_s) of ~300 K. Although electronically nonadiabatic effects are not included, we see an obvious difference in the two cases. NO($v_i = 16, E_i = 0.52$ eV) scattering from Au(111) undergoes multiquantum vibrational relaxation, yielding a broad vibrational state distribution down to $v_f \approx 2$ and peaking at $v_f \approx 10$. This amounts roughly to half of the experimentally measured vibrational relaxation [21]. Our recent work showed that the agreement with experiment in this and other conditions can be greatly improved further (see Fig. 2), if hot-electron effects were taken into account by the electronic friction theory with the orbital-dependent friction tensor (scaled to reasonably correct the Markovian approximation [36]). On the contrary, our calculations predict absolute vibrational elasticity of NO($v_i = 12$, $E_i = 0.42$ eV) scattered from LiF(001), in good accord

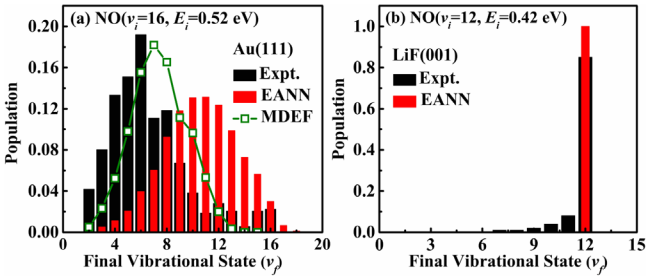

FIG. 2. Comparison of vibrational state distributions of highly vibrationally excited NO scattered from (a) Au(111) and (b) LiF (001), including the adiabatic QCT results on the EANN PES (red), nonadiabatic molecular dynamics with electronic friction (MDEF) results with the scaled orbital-dependent friction tensor taken from Ref. [36] (green), and experimental data (black). Initial conditions are selected mimicking the corresponding experiments.

TABLE I. Average rotational, vibrational, translational, and total energy losses (in eV) of NO before and after scattering from LiF(001) and Au(111) in various initial conditions (see text).

	LiF(001)		Au(111)	
Mean energy loss (eV)	NO($v_i = 12$) $E_i = 0.42$ eV	NO($v_i = 1$) $E_i = 0.31$ eV	NO($v_i = 16$) $E_i = 0.52$ eV	NO($v_i = 1$) $E_i = 0.31$ eV
$\langle \Delta E_{\mathrm{rot}} \rangle$	0.035	0.037	0.40	0.055
$\langle \Delta E_{\mathrm{vib}} \rangle$	−0.0010	−0.0013	−1.0	−0.0020
$\langle \Delta E_{\mathrm{trans}} \rangle$	−0.24	−0.10	−0.036	−0.13
$\langle \Delta E_{\mathrm{tot}} \rangle$	−0.20	−0.063	−0.65	−0.077

with the high survival probability observed in experiment. Apparently, the much more significant vibrational relaxation of highly vibrationally excited NO from Au(111) than from LiF(001) cannot be explained by the direct vibration-phonon coupling. Figure S5 [44] shows that phonon frequencies of LiF(001) are generally several times higher than those of Au(111), relatively closer to the NO vibrational frequency (1906 cm^{-1}). This should enable faster vibrational relaxation rate of NO on LiF(001) in terms of the energy gap law for vibrational energy transfer [28].

Different adiabatic energy transfer dynamics in the two cases can be further seen in the energy partitioning of scattered molecules. Table I compares the mean values of the rotational ΔE_{rot}, vibrational $\langle \Delta E_{\mathrm{vib}} \rangle$, translational $\Delta E_{\mathrm{trans}}$, and total energy loss $\langle \Delta E_{\mathrm{tot}} \rangle$ of NO scattering from LiF(001) and Au(111), defined by the final energy minus the initial energy of NO. Although there is negligible vibrational energy loss of NO($v_i = 12$) on LiF(001), about half of the translational energy is lost to the lattice, along with slight rotational excitation. This indicates that molecular vibration is barely coupled to other molecular and surface d.o.f., originating from the purely repulsive, nearly isotropic, and flat PES in this system (see Fig. 1 and Supplemental Material, Figs. S2–S4). To illustrate this more explicitly, a representative trajectory of NO($v_i = 12$, $E_i = 0.42$ eV) scattering from LiF(001) is projected onto Fig. 1(a). The vibrational motion is completely orthogonal to translation, whose amplitude is basically unperturbed upon the direct scattering process. Figure 3(a) further shows that the mechanical energy exchange between molecular translation and the LiF lattice occurs upon a short contact with the surface. The NO molecule quickly converts all of its translational energy to potential energy at the repulsive wall, then gets only half of the kinetic energy back when recoiling from the surface, resulting in a net translational energy loss to surface phonons. Interestingly, this calculated vibrational elasticity of NO scattering from LiF(001) is insensitive to the incidence energy, initial state, surface temperature, and even density functional (Fig. S6 [44]), as long as NO undergoes more or less the same repulsive force. Indeed, we find again no vibrational deexcitation of NO($v_i = 1$) scattered from LiF(001) at $E_i = 0.31$ eV, in-line with the large survival probability in experiment ($\sim 0.9 \pm 0.1$) in the same condition [22]. The average final translational energy of scattered molecules is ~0.21 eV, which compares well with the experimental value (~0.19 eV) [22]. The measured narrow angular distributions and rotational distributions [22,23] are also reasonably reproduced (Fig. S7 [44]). These results suggest that the scattering dynamics of NO from LiF(001) is well described by the new PES.

In sharp contrast, NO($v_i = 16, E_i = 0.52$ eV) scattered from Au(111) loses a substantial amount of vibrational energy ($\langle \Delta E_{\mathrm{vib}} \rangle = -1.0$ eV) and only a little translational energy ($\langle \Delta E_{\mathrm{trans}} \rangle = -0.036$ eV), flowing primarily into the lattice ($\langle \Delta E_{\mathrm{tot}} \rangle = -0.65$ eV) and partly to rotation ($\langle \Delta E_{\mathrm{rot}} \rangle = 0.40$ eV). Unlike the NO/LiF(001) case, now the highly vibrating NO molecule has an opportunity to lengthen and dissociate on Au(111) [35], during which the molecular vibration can gradually soften and thus couple with other d.o.f. Figure S8 [44] demonstrates the mode softening from 1906 cm^{-1} in the gas phase to 457 cm^{-1} at the transition state along the minimum energy path. Similar mode softening has effectively lowered the vibrationally

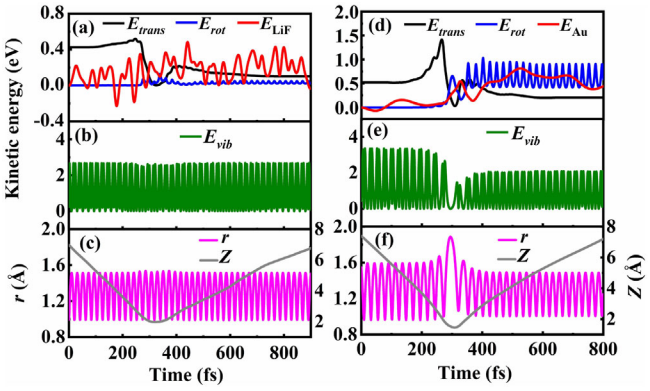

FIG. 3. Kinetic energy and geometric evolutions as a function of time during a representative scattering trajectory for (a)–(c) NO($v_i = 12, E_i = 0.42$ eV) from LiF(001) and (d)–(f)NO($v_i = 16, E_i = 0.52$ eV) from Au(111), including the kinetic energy in NO translation (E_{trans}, black), rotation (E_{rot}, blue), and vibration (E_{vib}, green), the average kinetic energy of surface atoms relative to the initial value (E_{LiF} and E_{Au}, red), the N-O distance (r, magenta), and the molecular height (Z, gray).

adiabatic barrier height and enabled great vibrational enhancement of dissociative adsorption of polyatomic molecules at metal surfaces [56]. Its influence on vibrationally inelastic scattering is clearly seen via a representative trajectory of $\mathrm{NO}(v_i = 16 \rightarrow v_f = 10)$ scattering from Au(111) in Fig. 1) and the corresponding kinetic energy evolution in each degree of freedom as a function of time in Figs. 3). In this case, before the first impact at the surface ($Z > 2.0$ Å), the NO molecule has acquired additional translational energy by ~0.89 eV with its bond length slightly extended to ~1.65 Å. Note that the NO-Au(111) attraction may accelerate the NO molecule by at most ~0.39 eV (i.e., the maximum adsorption well depth), but the excess translational energy gain must be transferred from vibration.

As the molecule goes more deeply to the repulsive wall and elongates further to the transition state region, the vibration is more significantly softened and the translation is suppressed. Both the vibrational kinetic energy and translational energy largely decrease, accompanied with a rapid increase of the kinetic energy of surface atoms (of course, also the potential energy of the system, which is, however, inseparable). Meanwhile, a large amount of energy is transferred to molecular rotation because the PES in this region features strong anisotropy and corrugation (Figs. S2–S4) and the molecule would reorient to resemble the transition state geometry. Another possible mechanism is that the larger bond length increases the molecule's moment of inertia, decreasing the rotational energy spacings and facilitating the rotational excitation [57]. Whatever the case is, molecule is eventually scattered back to the vacuum with much reduced vibrational excitation. Interestingly, even running calculations with all surface atoms fixed, we still see significant vibrational energy loss ($\Delta E_{\mathrm{vib}} = -0.71$ eV) of NO scattered from Au (111), but with a net average energy gain in translation ($\langle \Delta E_{\mathrm{trans}} \rangle = 0.22$ eV) and rotation ($\langle \Delta E_{\mathrm{rot}} \rangle = 0.49$ eV). This signifies that a large fraction of translational energy and part of rotational energy transferred from vibration eventually flows to surface phonons in the strongly interacting region when the surface is relaxed (Table S1 [44]).

We emphasize that such efficient adiabatic vibrational energy transfer would happen for highly vibrationally excited states of NO on Au(111) only. Indeed, the scattering of $\mathrm{NO}(v_i = 1, E_i = 0.31$ eV) from Au(111) turns out to be more similar to that from LiF(001), giving rise to nearly no vibrational energy loss (see Table I). Moreover, the mean translational energy loss of NO is 0.13 eV on Au(111), comparable to that on LiF(001). As illustrated in Fig. S9 [44], this is because $\mathrm{NO}(v_i = 1)$ cannot reach the dissociation channel on Au(111) and directly scatters in the entrance channel, manifesting a similar behavior as on the repulsive LiF(001) surface. We have found that mechanical vibrational deexcitation becomes measurable for $\mathrm{NO}(v_i = 3)$ and increasingly significant as E_i increase [35], as the molecule is more strongly affected by the force of the transition state region. The influence of a lengthening of the molecular bond on gas-surface scattering was first discussed by Jackson in model systems [57], assuming no particular barrier height, and subsequently discussed in more realistic systems with relatively low barriers and for low-vibrational states [4,6,58,59]. Our results highlight that the scattering of highly vibrationally excited molecules from solid surfaces can be strongly affected by a dissociation channel even when the barrier is very high and customarily ignored. This explains the negligible vibrational relaxation in adiabatic dynamics calculations on the empirical PES without a dissociation barrier [31].

With this more quantitative understanding of vibrational relaxation at gas-surface interfaces, we turn to discuss the remaining discrepancy between theory and experiment for $\mathrm{NO}(v_i = 12)$ scattering from LiF(001). Defects in experimentally prepared LiF(001) samples have been invoked to explain the observed minor vibrational inelasticity of $\mathrm{NO}(v_i = 12)$ [23]. The influence of defects can be remarkable, for example, $\mathrm{NO}(v_i = 1)$ scattering was found completely vibrationally inelastic [60] from polished LiF (001) (with possibly high concentration of defects), while mostly vibrationally elastic [22] from well-cleaved LiF (001). By performing additional DFT calculations on defective LiF(001) surfaces with steps or ionic vacancies (Figs. S11–S13 [44]), we find that those defects only moderately strengthen the NO-LiF binding, but fail to support any dissociation transition states. Based on our analysis, however, the mechanical vibrational relaxation would be significant only if the repulsive PES was largely changed to enable some sort of chemical transformation. On the other hand, we find that a single Li^+ vacancy can significantly reduce the band gap of LiF(001) to ~2.40 eV, which may be accessible by $\mathrm{NO}(v_i = 12)$ with a vibrational energy of ~2.70 eV. Additional work is needed to learn whether this would cause some nonadiabatic vibrational energy loss of NO on imperfect LiF(001).

To summarize, we present a comparative study on the adiabatic energy transfer dynamics of NO scattering from Au(111) and LiF(001) revealed by high-dimensional global neural network PESs with DFT accuracy. We find almost exclusive vibrationally elastic products of $\mathrm{NO}(v_i = 12)$ scattered from LiF(001), in stark contrast with the multiquantum relaxation $\mathrm{NO}(v_i = 16)$ from Au(111). However, the scattering of $\mathrm{NO}(v_i = 1)$ from both surfaces is vibrationally elastic and only translational energy leads to phonon excitation. This interesting discrepancy and similarity have been quantitatively rationalized by the potential energy landscape accessible by the impinging NO molecule. As long as the molecule reaches the dissociation barrier region, its vibration will be significantly softened and energy transfer from vibration to translation, rotation, and phonons is significant. When the low-vibrating NO

molecule is rejected directly without experiencing the dissociative force and the vibrational softening on Au(111), it manifests a similar behavior as on the purely repulsive LiF(001) surface. Our results not only reproduce well the experimental data for NO scattering on LiF(001), but also suggest a mechanical mechanism for the discrepant vibrational relaxation of highly vibrating NO scattering from metallic and insulating surfaces. An apparent next step is to combine this mechanical and the electron-mediated nonadiabatic vibrational energy transfer channels, which could be both promoted by the same region of the PES [24], to fully understand the energy transfer dynamics of molecules like NO and CO at metal surfaces.

We appreciate the support from National Key R&D Program of China (2017YFA0303500), National Natural Science Foundation of China (22073089 and 22033007), and Anhui Initiative in Quantum Information Technologies (AHY090200). We thank Professor Alec Wodtke for some helpful discussions. The Fundamental Research Funds for the Central Universities (WK2060000017). We appreciate the Supercomputing Center of USTC for high-performance computing services.

*bjiangch@ustc.edu.cn

[1] G. B. Park, B. C. Krüger, D. Borodin, T. N. Kitsopoulos, and A. M. Wodtke, Rep. Prog. Phys. **82**, 096401 (2019).
[2] C. T. Rettner, F. Fabre, J. Kimman, and D. J. Auerbach, Phys. Rev. Lett. **55**, 1904 (1985).
[3] B. D. Kay, T. D. Raymond, and M. E. Coltrin, Phys. Rev. Lett. **59**, 2792 (1987).
[4] C. T. Rettner, D. J. Auerbach, and H. A. Michelsen, Phys. Rev. Lett. **68**, 2547 (1992).
[5] K. Golibrzuch, P. R. Shirhatti, J. Altschaffel, I. Rahinov, D. J. Auerbach, A. M. Wodtke, and C. Bartels, J. Phys. Chem. A **117**, 8750 (2013).
[6] J. Geweke, P. R. Shirhatti, I. Rahinov, C. Bartels, and A. M. Wodtke, J. Chem. Phys. **145**, 054709 (2016).
[7] J. Werdecker, M. E. van Reijzen, B.-J. Chen, and R. D. Beck, Phys. Rev. Lett. **120**, 053402 (2018).
[8] L. Martin-Gondre, M. Alducin, G. A. Bocan, R. Díez Muiño, and J. I. Juaristi, Phys. Rev. Lett. **108**, 096101 (2012).
[9] G.-J. Kroes and C. Diaz, Chem. Soc. Rev. **45**, 3658 (2016).
[10] Z. Zhang, T. Liu, B. Fu, X. Yang, and D. H. Zhang, Nat. Commun. **7**, 11953 (2016).
[11] M. Alducin, R. Díez Muiño, and J. I. Juaristi, Prog. Surf. Sci. **92**, 317 (2017).
[12] P. Spiering and J. Meyer, J. Phys. Chem. Lett. **9**, 1803 (2018).
[13] L. Zhang and B. Jiang, Phys. Rev. Lett. **123**, 106001 (2019).
[14] Y. Huang, C. T. Rettner, D. J. Auerbach, and A. M. Wodtke, Science **290**, 111 (2000).
[15] Y. Huang, A. M. Wodtke, H. Hou, C. T. Rettner, and D. J. Auerbach, Phys. Rev. Lett. **84**, 2985 (2000).
[16] R. Cooper, C. Bartels, A. Kandratsenka, I. Rahinov, N. Shenvi, K. Golibrzuch, Z. Li, D. J. Auerbach, J. C. Tully, and A. M. Wodtke, Angew. Chem., Int. Ed. Engl. **51**, 4954 (2012).
[17] K. Golibrzuch, P. R. Shirhatti, J. Altschaffel, I. Rahinov, D. J. Auerbach, A. M. Wodtke, and C. Bartels, J. Phys. Chem. A **117**, 8750 (2013).
[18] N. Bartels, B. C. Kruger, D. J. Auerbach, A. M. Wodtke, and T. Schafer, Angew. Chem., Int. Ed. Engl. **53**, 13690 (2014).
[19] K. Golibrzuch, P. R. Shirhatti, I. Rahinov, A. Kandratsenka, D. J. Auerbach, A. M. Wodtke, and C. Bartels, J. Chem. Phys. **140**, 044701 (2014).
[20] K. Golibrzuch, N. Bartels, D. J. Auerbach, and A. M. Wodtke, Annu. Rev. Phys. Chem. **66**, 399 (2015).
[21] B. C. Kruger, N. Bartels, C. Bartels, A. Kandratsenka, J. C. Tully, A. M. Wodtke, and T. Schafer, J. Phys. Chem. C **119**, 3268 (2015).
[22] J. Misewich, H. Zacharias, and M. M. T. Loy, Phys. Rev. Lett. **55**, 1919 (1985).
[23] A. M. Wodtke, Y. Huang, and D. J. Auerbach, J. Chem. Phys. **118**, 8033 (2003).
[24] B. C. Krüger, S. Meyer, A. Kandratsenka, A. M. Wodtke, and T. Schäfer, J. Phys. Chem. Lett. **7**, 441 (2016).
[25] N. Bartels, K. Golibrzuch, C. Bartels, L. Chen, D. J. Auerbach, A. M. Wodtke, and T. Schafer, J. Chem. Phys. **140**, 054710 (2014).
[26] A. M. Wodtke, D. Matsiev, and D. J. Auerbach, Prog. Surf. Sci. **83**, 167 (2008).
[27] A. M. Wodtke, Chem. Soc. Rev. **45**, 3641 (2016).
[28] R. R. Lucchese and J. C. Tully, J. Chem. Phys. **80**, 3451 (1984).
[29] S. Li and H. Guo, J. Chem. Phys. **117**, 4499 (2002).
[30] N. Shenvi, S. Roy, and J. C. Tully, J. Chem. Phys. **130**, 174107 (2009).
[31] N. Shenvi, S. Roy, and J. C. Tully, Science **326**, 829 (2009).
[32] S. Monturet and P. Saalfrank, Phys. Rev. B **82**, 075404 (2010).
[33] S. Roy, N. A. Shenvi, and J. C. Tully, J. Chem. Phys. **130**, 174716 (2009).
[34] J. Misewich, H. Zacharias, and M. M. T. Loy, J. Vac. Sci. Technol. B **3**, 1474 (1985).
[35] R. Yin, Y. Zhang, and B. Jiang, J. Phys. Chem. Lett. **10**, 5969 (2019).
[36] C. L. Box, Y. Zhang, R. Yin, B. Jiang, and R. J. Maurer, JACS Au **1**, 164 (2020).
[37] G. Kresse and J. Furthmuller, Phys. Rev. B **54**, 11169 (1996).
[38] G. Kresse and J. Furthmuller, Comput. Mater. Sci. **6**, 15 (1996).
[39] J. P. Perdew, J. A. Chevary, S. H. Vosko, K. A. Jackson, M. R. Pederson, D. J. Singh, and C. Fiolhais, Phys. Rev. B **46**, 6671 (1992).
[40] Y. Zhang, X. Zhou, and B. Jiang, J. Phys. Chem. Lett. **10**, 1185 (2019).
[41] Y. Zhang, C. Hu, and B. Jiang, J. Phys. Chem. Lett. **10**, 4962 (2019).
[42] L. Zhu, Y. Zhang, L. Zhang, X. Zhou, and B. Jiang, Phys. Chem. Chem. Phys. **22**, 13958 (2020).
[43] Y. Zhang, R. J. Maurer, and B. Jiang, J. Phys. Chem. C **124**, 186 (2020).
[44] See Supplemental Material at http://link.aps.org/supplemental/10.1103/PhysRevLett.126.156101 for details

of computational methods and additional results, which includes Refs. [9,14,17–19,21,23,35–38,40–43, 45–55].
[45] J. P. Perdew, K. Burke, and M. Ernzerhof, Phys. Rev. Lett. **77**, 3865 (1996).
[46] P. E. Blöchl, Phys. Rev. B **50**, 17953 (1994).
[47] H. J. Monkhorst and J. D. Pack, Phys. Rev. B **13**, 5188 (1976).
[48] J. Klimeš, D. R. Bowler, and A. Michaelides, J. Phys. Condens. Matter **22**, 022201 (2010).
[49] S. F. Boys and A. C. Egerton, Proc. R. Soc. A **200**, 542 (1950).
[50] J. Behler, J. Chem. Phys. **134**, 074106 (2011).
[51] W.-K. Chen, Y. Zhang, B. Jiang, W.-H. Fang, and G. Cui, J. Phys. Chem. A **124**, 5684 (2020).
[52] W. L. Hase, R. J. Duchovic, X. Hu, A. Komornicki, K. F. Lim, D.-H. Lu, G. H. Peslherbe, K. N. Swamy, S. R. V. Linde, A. Varandas, H. Wang, and R. J. Wolfe, Quantum Chem. Program Exchange Bull. **16**, 671 (1996), http://hase-group.ttu.edu/venus/venus96_manual.html.
[53] W. L. Hase, in *Encyclopedia of Computational Chemistry*, edited by N. L. Alinger (Wiley, New York, 1998), pp. 399.
[54] M. C. Gutzwiller, *Chaos in Classical and Quantum Mechanics* (Springer, New York, London, 1990).
[55] L. Bonnet, Int. Rev. Phys. Chem. **32**, 171 (2013).
[56] S. Nave, A. K. Tiwari, and B. Jackson, J. Phys. Chem. A **118**, 9615 (2014).
[57] B. Jackson, J. Phys. Chem. **93**, 7699 (1989).
[58] M. del Cueto, X. Zhou, A. S. Muzas, C. Díaz, F. Martín, B. Jiang, and H. Guo, J. Phys. Chem. C **123**, 16223 (2019).
[59] J. Werdecker, B.-J. Chen, M. E. Van Reijzen, A. Farjamnia, B. Jackson, and R. D. Beck, Phys. Rev. Research **2**, 043251 (2020).
[60] H. Zacharias, M. M. T. Loy, and P. A. Roland, Phys. Rev. Lett. **49**, 1790 (1982).